Available online at www.sciencedirect.com
SCIENCE DIRECT
Cryogenics 46 (2006) 9–20
Cryogenics
www.elsevier.com/locate/cryogenics

A sorption compressor with a single sorber bed for use with a Linde–Hampson cold stage

G.F.M. Wiegerinck, J.F. Burger, H.J. Holland, E. Hondebrink, H.J.M. ter Brake *, H. Rogalla

Low Temperature Division, Faculty of Science and Technology, University of Twente, P.O. Box 217, 7500 AE Enschede, The Netherlands

Received 25 January 2005; received in revised form 3 February 2005; accepted 26 August 2005

Abstract

A sorption compressor cell basically consists of a container that is filled with an adsorbent. When such a cell is thermally cycled, a pressure difference is created by the subsequent adsorption and desorption of the gas. As a consequence, a single sorption compressor cell inherently provides an intermittent flow. A Joule–Thomson expansion stage requires a more or less continuous flow. The standard way to obtain a continuous flow out of a sorption compressor is to use three or more compressor cells that are operated out of phase. This paper presents an alternative compressor concept that uses only one compressor cell, two buffer volumes and two check valves. Such a compressor is easier to construct and to operate and has a higher reliability at the expense of a slight variation in the cooler's cold-end temperature. The principle was demonstrated using a sorption compressor cell that is filled with Maxsorb [The Kansai Coke & Chemicals Co. Ltd., 1-1 Oh-Hama, Amagasaki, Japan 660] activated carbon, is equipped with a gas-gap heat switch, and uses xenon as the working fluid. A flow of 0.52 mg/s was achieved with a low pressure of 1.39 bar and a high pressure of 17.0 bar, giving a theoretical cooling power of 42 mW at 172 K. A sensitivity analysis on several control parameters has been performed experimentally.

Keywords: Sorption coolers; Joule–Thomson coolers; Xenon

1. Introduction

A sorption compressor cell basically consists of a container that is filled with an adsorbent. It can act as a compressor by thermally cycling the adsorbent and at the same time controlling the gas flow to and from the system. One can distinguish four different parts in the cycle. These are schematically shown in Fig. 1. Starting from an initial low (heat sink) temperature and pressure (point 1), during the first part of the cycle (A) the sorber container is heated while no gas can flow into or out off the compressor cell. Adsorbed gas comes off the surface and builds up pressure in the void volume. As a consequence, the adsorbed amount of gas per gram of sorber material x_s decreases while the pressure increases. During this phase, the total amount of gas in the sorber container remains constant. When the container is opened (point 2), high-pressure gas flows out (phase B). The pressure in this phase is determined by the mass flow rate out off the compressor and the rate of desorption. In Fig. 1, a constant pressure is assumed. When most of the gas has come off the surface (point 3), the container is cooled back to the heat sink temperature and the container is closed (phase C). Gas from the void volume now adsorbs onto the surface of the sorber material, causing the pressure in the container to drop. At a sufficiently low pressure (point 4), gas should be supplied to the sorber container in order to return to the starting point (phase D). The pressure in the cell during this phase depends on the mass flow rate of the gas flowing into the compressor and the rate of adsorption. So, during only one phase of the cycle (phase B) high-pressure gas is supplied by the cell and during another phase (phase D)

* Corresponding author. Tel.: +31 53 489 4349; fax: +31 53 489 1099.
E-mail address: h.j.m.terbrake@utwente.nl (H.J.M. ter Brake).

0011-2275/$ - see front matter © 2005 Elsevier Ltd. All rights reserved.
doi:10.1016/j.cryogenics.2005.08.006

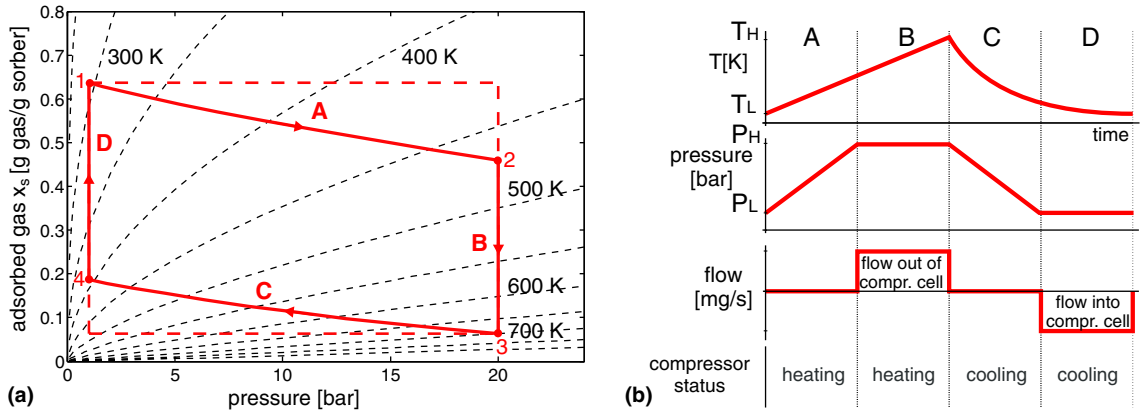

Fig. 1. (a) Amount of adsorbed xenon per gram of sorber material during the sorption cycle for Maxsorb activated carbon. The dashed lines are sorption isotherms. (b) Temperature, pressure, flow, and compressor status with time during the sorption cycle.

low-pressure gas is taken up by the cell. In the other two phases no gas flows into or out off the system. Whereas an individual sorption cell provides an intermittent flow, a Joule–Thomson (JT) expansion stage needs a more or less continuous mass flow in order to provide continuous cooling power. In general, a continuous flow is obtained by using three or more compressor cells. They are operated out of phase and their phases are synchronised. A set of valves is used to convert the intermittent flows of the individual cells to a continuous flow through the cold stage. A schematic picture of such a cooler using four sorption cells is shown in Fig. 2. Bowman et al. [2] recently published an overview of closed-cycle JT cryocoolers.

Coolers that consist of a sorption compressor with a Linde–Hampson (LH) cold stage have several advantages. They are thermally driven and have no moving parts, apart from some valves. As a consequence, they can be scaled to small sizes and can operate with an absolute minimum vibration level. Besides, wear-related issues hardly play a role giving the potential for a long cooler lifetime.

A disadvantage of this cooler type is the relatively complex compressor design including three or more compressor cells, each consisting of a container filled with sorber material and equipped with a heater, a heat switch with an actuator, and some means to control the heater and the heat switch actuator. As more complicated components in a system increase the risk of failures, a reduction of complexity would increase the reliability of the cooler.

In the next section, we present an alternative design to create a continuous flow with a single compressor cell thus significantly reducing the complexity of the system. Section 3 describes the design of the set-up that was used to demonstrate the proposed compressor configuration. The functioning of the set-up is described in Section 4. The first part of this section describes the time-dependent behaviour of pressures and mass flows in the system. This paper only addresses the compressor part of the cooler. Therefore, Section 4 includes a discussion on the expected implications of the compressor design on the cold stage. Besides, the

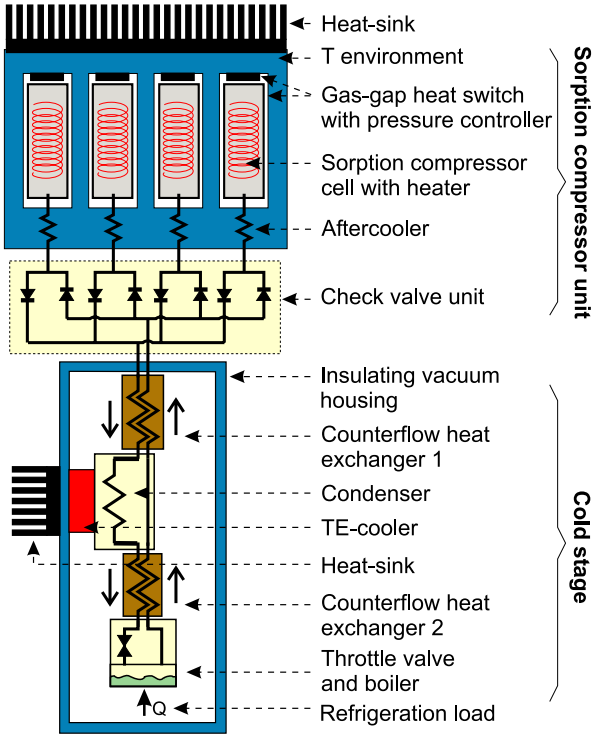

Fig. 2. Sorption compressor with a Linde–Hampson cold stage using four sorption compressor cells operating 90° out of phase. For more information, see e.g. [10].

experimental results of a sensitivity analysis on the most important control parameters are described. The paper ends with conclusions on the proposed compressor design.

2. Single-cell compressor

A JT expansion stage requires a more or less continuous mass flow in order to obtain a continuous cooling power. Besides, the compressor should supply a constant low pressure as this pressure is directly related to the low-end temperature of the cold stage. As set out in the previous

section, a single sorption cell supplies an inherently non-continuous flow. An alternative to using multiple compressor cells to get a continuous flow is a compressor unit that uses only a single sorption compressor cell and two buffer volumes separated by passive valves. This design is shown in Fig. 3. A similar design was applied by Duband and Suhanan [3,4], but they did not analyse the concept in detail.

During phase A of the sorption cycle, the sorber container is heated and pressure builds up in the sorber container as both check valves are closed because of the pressure differences over the valves. The high-pressure buffer supplies gas to the cold stage which is taken up by the low-pressure buffer, while no gas flows to or from the compressor cell. As a consequence, the pressure of the high-pressure buffer slowly decreases while that of the low-pressure buffer steadily increases. Once the pressure in the container has become higher than that of the high-pressure buffer, the high-pressure check valve opens and a relatively large gas flow is supplied to the high-pressure buffer, causing the pressure of that buffer to rise (phase B). When the container is cooled down, the pressure in the container decreases and the high-pressure check valve closes (phase C). Again, the flow through the cold stage is maintained by the buffers. When the pressure in the container has dropped to below that of the low-pressure buffer, the low-pressure check valve opens and gas flows from the buffer to the cell (phase D).

This configuration has important advantages. First of all, the number of components is reduced. This increases the reliability of the compressor. Besides, controlling the cooler is easier as only one sorption compressor cell needs to be driven. The reliability of the design can be further increased by mounting a second compressor cell between the low-pressure and high-pressure buffers. The 2 parallel cells can be operated independently. If one of the compressor cells fails, the compressor can still operate (redundancy). The advantage of reduction of complexity becomes even more pronounced when multi-staged compression is applied as suggested by Bard [5]. With a two-stage compression approach, the COP of the cooler can be increased. Then, instead of two compressor units consisting of at least six sorption compressor cells and 12 check valves, only two sorption compressor cells, three buffer volumes and four check valves are needed. Besides, in the proposed lay-out no synchronisation between the different compressor cells is needed. As a result, each cell can be cycled at its optimum cycle frequency, and does not have to be tuned to others as is the case in the traditional lay-out. The cycle time will also be shorter. Therefore, the single-cell design provides a larger mass flow per cell than in the traditional design, assuming that the cell pumps the same amount of gas from the low-pressure to the high-pressure side during a cycle. A disadvantage of the proposed design compared to the traditional lay-out is the slight fluctuation in pressure of the low-pressure buffer. This will result in some variation of the cold stage temperature. Proper design of the low-pressure buffer can minimise this temperature variation. Furthermore, this temperature fluctuation can be damped passively or actively. Another disadvantage of the pressure fluctuations in the buffers is that both the flow through the cold stage and the enthalpy of cooling will slightly vary with time as shown with some exaggeration in Fig. 3. However, the actual cooling power of the cold stage is buffered by the evaporating liquid in the boiler.

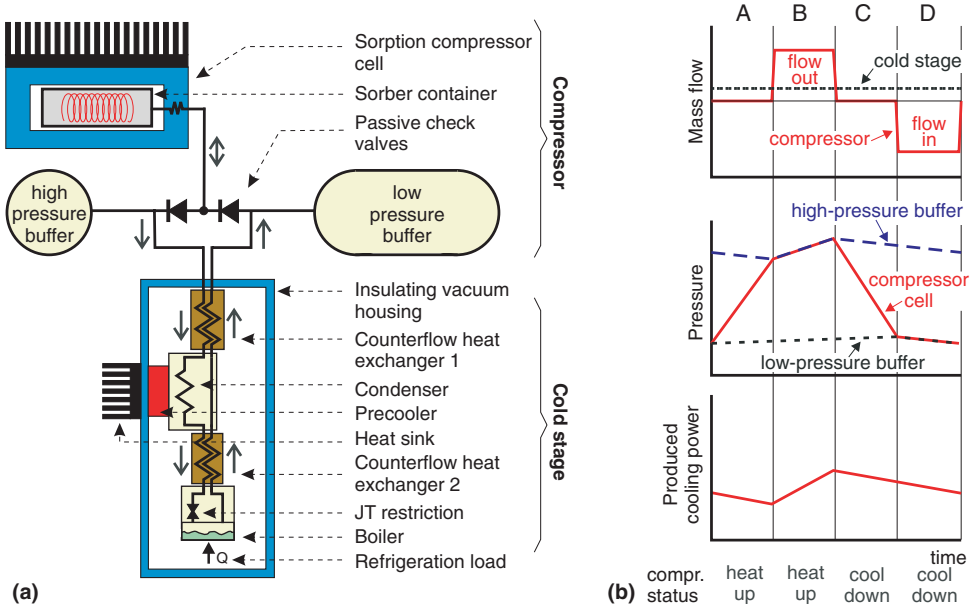

Fig. 3. Single-cell sorption compressor combined with a LH cold stage. (a) Schematic drawing of the configuration. (b) Mass flow, pressure, and produced cooling power (exaggerated vertical scale) with time.

3. System description

3.1. Thermodynamical set points

To demonstrate the single-cell sorption compressor, we selected xenon as the working fluid. This gas adsorbs reasonably well at room temperature while at the same time a relatively low temperature of 165 K can be reached for a compressor low pressure of 1 bar. To liquefy the fluid in the precooler, and hence increase the efficiency of the cold stage [6], the high-pressure gas should be precooled below the boiling point of the fluid at that pressure, e.g. by means of a 2-stage TE-cooler [7]. For xenon, this implies a compressor high pressure in the range of 16–19 bar when the gas is precooled to 235–240 K. Of course, the selection of the working fluid and the thermodynamic setpoints is rather arbitrary. Also other gases can be taken depending on the requirements of the cooler.

To test the compressor performance, the experiments were performed without a cold stage. Instead, a tunable needle valve was used to establish the required pressure drop. Section 4.2 gives a theoretical description of the expected behaviour of a LH cold stage, if it was connected to the compressor type under investigation.

3.2. Sorption compressor cell

The design of the compressor cell is shown schematically in Fig. 4. The cell consists of a container that is filled with a sorber material. The sorber container has an inner diameter of 9.4 mm and a length of 10 cm. It was filled with commercially available Maxsorb MSC-30 activated carbon [1]. This sorber material has a surface area of 3290 m^2/g and an apparent density of 0.28 g/ml [1,8]. The charcoal was filtered and particles with a diameter between 210 and 420 μm were selected. The void volume between the filter of the sorption compressor cell and the check valves is estimated at 0.8 cm^3. The internal void volume is about 6 cm^3. Application of other activated carbons with inherently lower void volume fractions would improve the pressure swing that can be achieved as less gas is lost in the void volume. However, such a sorber is not needed to demonstrate the operation of the single-cell compressor. The sorber container is closed by a 2 μm stainless steel filter. In this filter, a feedthrough for an Omega [9] E-type thermocouple was welded. This thermocouple is used both for measuring the temperature and as a heating element. While thermally cycling the sorber container, the thermocouple is switched between the heating mode and the measuring mode. The sorber container is gold-plated to reduce radiative heat loss and it is centred in a stainless steel heat sink by means of two spacers. For a more detailed description of the compressor cell, the reader is referred to Burger et al. [10].

The sorption compressor cell from Fig. 4 was heat sinked at 20 °C. The pressure in the sorber container is measured outside the cell with a low void-volume Kulite pressure sensor (type XTL-190) [11]. The temperature of the heat sink and of the 'cold junction' of the thermocouple was monitored with Heraeus PT1000-resistors [12].

3.3. Gas-gap heat switch

In principle, a sorption compressor can be realised with a fixed thermal resistance between the sorber container and the heat sink. Then, the selected resistance is a compromise between a large value for the heating phases and a small value for the cooling phases. Application of a heat switch therefore gives a larger compressor COP because less heat leaks to the heat sink during the heating phases. Of course, the input power of the heat switch actuator should not outweigh the increase in compressor COP. A fixed thermal resistance also results in a longer cycle time as the cool-down phase takes longer. For a compressor consisting of multiple compressor cells synchronisation between the cells is required. For such a design, the longer cool-down time can be compensated by using additional cells. For the single-cell design, this cannot be done and the absence of a heat switch directly results in a smaller pressure swing. This stresses the importance of the application of a heat switch for the compressor type under investigation.

As is shown in Fig. 4, we applied a gas-gap heat switch in our design. The heat transfer through such a gap

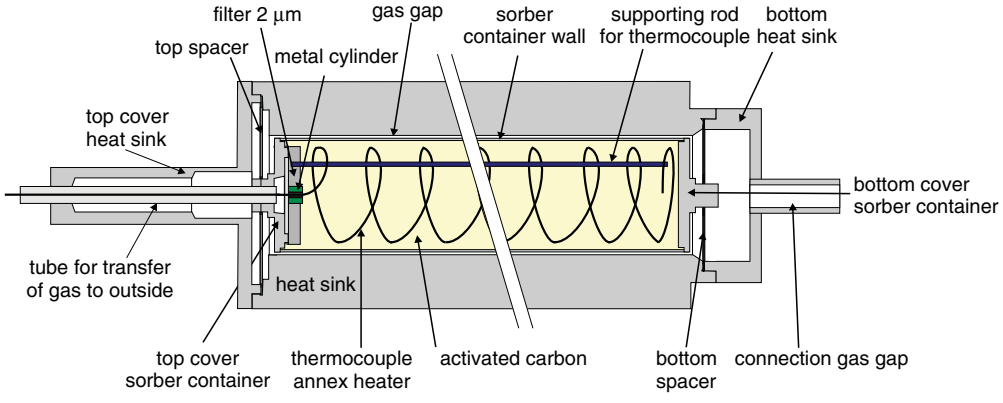

Fig. 4. Schematic drawing of the sorption compressor cell.

depends on the pressure in the gap, the dimensions of the gap and on the properties of the gas that is applied. The pressure dependence is used to switch the thermal contact [13–15]. A separate sorption compressor cell that is integrated in the gas-gap can be used as an actuator. This unit can e.g. be a metal-hydride acting as a sorber material with H_2 as the working gas [15,16]. To test the compressor operation in a laboratory set-up, we created the pressure swing in the gas-gap by switching the gas-gap volume between a low-pressure and a high-pressure 'reservoir' with the help of two active valves. This, and the other components of the experimental set-up, is shown schematically in Fig. 5. For safety reasons, we selected helium as the working gas despite the slightly worse heat transfer characteristics compared to hydrogen.

A gas-gap high pressure of 50 mbar was selected. At this pressure, the gas in the gap is nearly in the viscous regime. For the low-pressure, 5×10^{-4} mbar was taken. This is the lowest pressure the vacuum pump could achieve. The cool-down behaviour of the sorber container was measured for a range of pressures. From this, the pressure-dependent thermal resistance was determined. This was fitted to theory [13–15] by using the accommodation coefficient as the fitting parameter. For the selected pressures, the thermal resistance switches between 4×10^3 K/W during the heating phases and 0.5 K/W during the cooling phases. The pressures in both the high-pressure and the low-pressure reservoirs connected to the gap space were measured with MKS Baratron 627B pressure transducers [17].

3.4. Buffer volumes

The pressure variations in both buffers connected to the compressor cell depend on the mass flow through the needle valve, the cycle time and the volume as expressed in Eq. (1)

$$\Delta p = \frac{\dot{m}_{\mathrm{cool}} RT}{VM} (t_{\mathrm{cycle}} - t_{\mathrm{flow}}) \tag{1}$$

Here, Δp is the pressure variation in the buffer, $\dot{m}_{\mathrm{cool}}$ is the mass flow through the needle valve, R is the universal gas constant, T is the absolute temperature of the buffer, V is the buffer volume, M is the mole mass of the working fluid, t_{cycle} is the cycle time, and t_{flow} is the period during which there is a gas flow between the compressor cell and the buffer under consideration. This formula only holds for relatively small pressure variations. Furthermore, the flow through the restriction should not exceed the flow between the cell and the buffer. A volume of 300 cm^3 was selected for the low-pressure buffer and of 50 cm^3 for the high-pressure buffer.

3.5. Check valves

We used Swagelok 6L-CW4S4 valves [18] that have a cracking pressure of 11 mbar and a pressure drop of 22 mbar for a xenon flow of 4 mg/s at 1.3 bar. The pressure of the compressor cell rises with a rate of 0.075 bar/s during phase A of the sorption cycle. At this rate, in total 0.3 mg gas leaks through the valve before the leak flow falls below 1 μg/s, the noise level of the mass flow meter. This leak is acceptable compared to the total forward flow during a cycle, which is a few hundred milligrams. In phase C, the check valve on the high-pressure side closes when the pressure in the cell drops. Also here, the leak flow is smaller than the noise level of the sensor. To prevent pollution of the check valves, Valco filters with screens of 10 μm pore size are applied on both sides of the filter. A disadvantage of the selected check valves is their relatively large void volume. This was filled with metal, reducing it to about 0.1 cm^3 for each valve. An alternative approach would be to use microminiature check valves [19]. Such valves were not applied because of the time and cost of manufacturing,

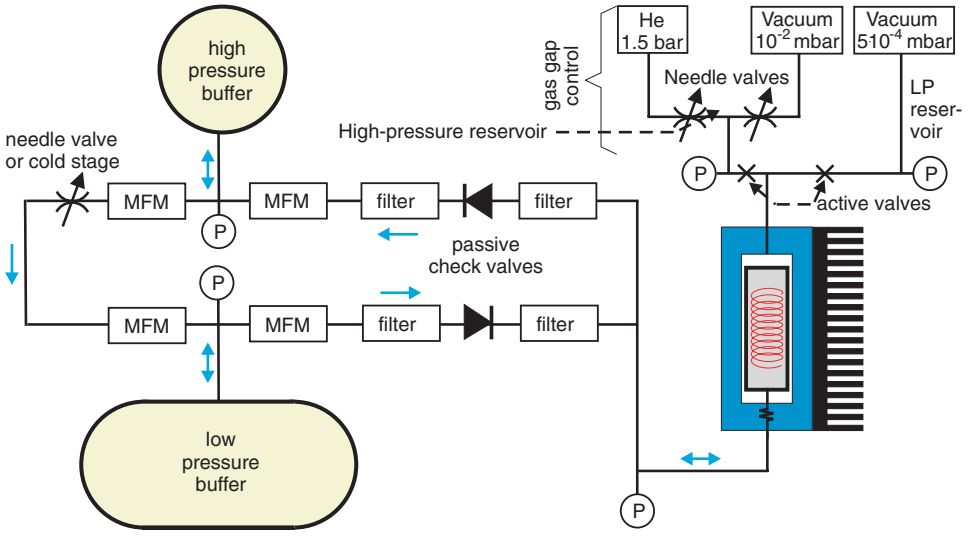

Fig. 5. Schematic overview of the experimental set-up. See text for details.

whereas low-dead volume valves are not essential to demonstrate the compressor concept.

3.6. System control algorithm and additional instrumentation

To obtain the maximum achievable pressure difference for a fixed value of the flow restriction, the compressor cell should pump as much as possible gas from the low-pressure buffer to the high-pressure buffer in an as short as possible cycle time. The heating phases can be sped up by increasing the compressor input power and the duty cycle, i.e. the fraction of time during which the thermocouple is switched to the heating mode. However, as the thermal conductivity of charcoal powder is low, fast heating implies a considerable temperature profile over the heater. It results from Fig. 1(a) that $\partial x_s/\partial T$ is negative and $\partial^2 x_s/\partial T^2$ is positive, with x_s being the amount of gas adsorbed per gram of sorber material. Then, a temperature profile over the sorber material results in less desorption compared to the case of a uniform temperature with the same energy input to the sorber. Although a temperature gradient is not necessarily problematic for the pressure swing, it can reduce the compressor efficiency dramatically. If one aims at a maximum pressure difference, the compressor cell should pump as much as possible gas from the low-pressure buffer to the high-pressure buffer in an as short as possible cycle time. In other words, the amount of gas that is pumped by the compressor during one cycle divided by the cycle time should be maximised. This means that the compressor should be switched from the heating mode to the cooling mode when the additional amount of gas flown to the high-pressure buffer does not compensate the additional cycle time that is needed. This is definitely the case when the flow to the high-pressure buffer becomes lower than the flow through the restriction. For a compressor design with a gas-gap heat switch, the fastest cool down rate is obtained when the gas in the gap is in the viscous state. Similar to the heating phases, the cooling should be continued until the additional amount of gas that flows to the cell does not compensate the additional time needed.

In our set-up we use a single spirally-wound heater. To limit the temperature profile and to perform the heating phase as fast as possible, the control algorithm initially heats the sorber container with a duty cycle of 85%. Each time the thermocouple is switched to the measuring mode, the observed temperature reduces rapidly as the heat distributes more uniformly over the sorber material. When the set maximum temperature is reached, the duty cycle is reduced by 5%. When the heater is switched on again, it will take some time before the set maximum temperature is reached again as the duty cycle has been reduced. Then, the duty cycle is again reduced by 5% and so on. The compressor is switched to the cooling mode when the flow to the high-pressure buffer has become smaller than a factor f_{BC} times the flow through the needle valve, with f_{BC} a constant that can be set in the control algorithm. During the cooling phase, the heater is switched off and the gas-gap is switched to the selected high pressure. Similar to the heating phase, the cooling is continued until the flow from the low-pressure buffer to the cell has become lower than a factor f_{DA} times the flow through the needle valve with f_{DA} again a constant which is set in the control algorithm.

The control algorithm was implemented in a LabVIEW programme [20]. The pressures of the high and low-pressure buffers are measured with Druck PTX1400 sensors [21]. The mass flows between the buffers and the sorption compressor cell and between the buffers and the flow restriction are measured with Bronkhorst EL-FLOW mass flow meters [22]. The data are sampled with a National Instruments multiplexer board connected to an E-series DAQ-card [20]. Each channel is sampled with 100 Hz and averaged over 50 samples before the data was further processed. The thermocouple data form an exception to this, as the moment, the thermocouple is switched between the heating and the measuring mode, is not synchronised with the start of the averaging intervals.

4. Results and discussion

4.1. Compressor operation

The compressor was operated for more than 200 cycles with f_{BC} set to 1.0, f_{DA} set to 1.2, a peak heater input power of 7.0 W, and a set maximum temperature of 700 K. The flow restriction was set at such a value that the high pressure was above 16 bar, the pressure needed to condense the gas in the precooler. We aimed at a value close to atmospheric pressure for the low-pressure side. The behaviour of the system during four typical cycles is shown in Fig. 6. The heat input averaged over the total cycle was 3.2 W. The pressure in the container alternated between 1.35 and 17.2 bar. The high-pressure buffer fluctuated between 16.4 and 17.0 bar and that of the low-pressure buffer varied between 1.39 and 1.53 bar. These pressure values varied less than 2% over the 200 cycles. The compressor heat-sink temperature was kept fixed at 293 K. The temperature of the other components varied slightly because of temperature fluctuations in the laboratory. The average mass flow through the flow restriction was 0.52 mg/s. The broad band in the mass flow from the cell to the high-pressure buffer is caused by the intermittent heating during phase B. The average periods of the phases in stable operation are 199 s for phase A, 159 s for phase B, 72 s for phase C, and 168 s for phase D. When applying Eq. (1) to these times, we obtain a pressure variation in the high-pressure buffer of 0.63 and 0.14 bar for the low-pressure buffer. This agrees well with the measurements described above.

If the cell from this set-up would be applied in a traditional set-up using 4 cells, the cycle time would increase to 796 s because of the synchronisation. Each cell would then, on average, deliver a flow of 0.39 mg/s to the restriction, assuming that the amount of gas that is pumped by the cell during a cycle does not change. The total flow

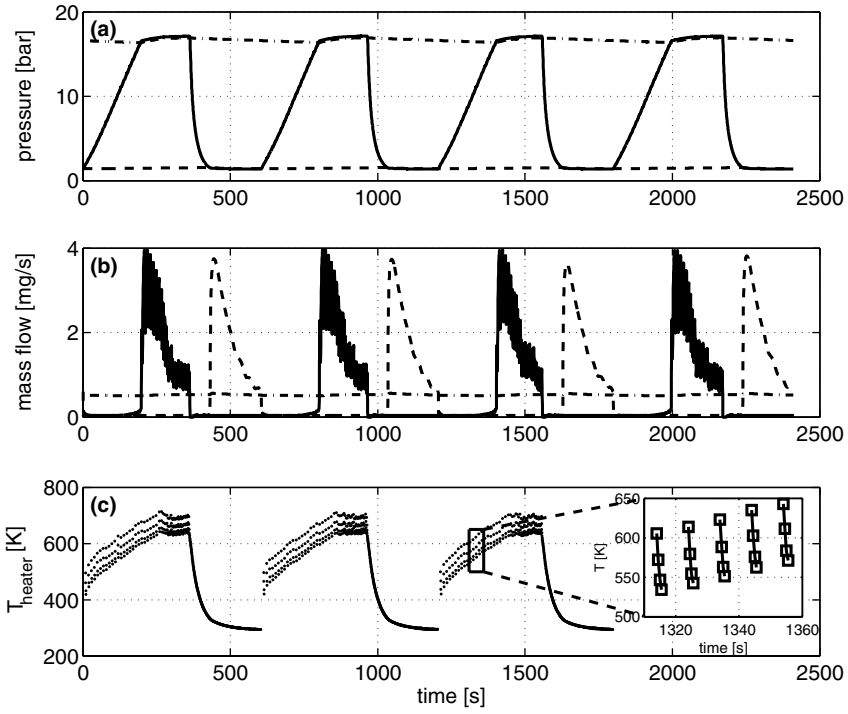

Fig. 6. Operation of a single-cell compressor (a) Pressure versus time; P_{cell} (solid), $P_{LP,buffer}$ (dashed), $P_{HP,buffer}$ (dash-dotted). (b) Mass flow versus time; cell to HP_{buffer} (solid), flow through restriction (dash-dotted), LP_{buffer} to cell (dashed). (c) T_{heater} versus time. The measured temperatures are shown as dots (see inset). In the heating mode, the temperature cannot be measured. In the measuring mode, the temperature of the thermocouple decreases because heat flows to the surrounding charcoal.

through the restriction would be 1.56 mg/s, three times that of the single-cell design. To get the same flow out off the single-cell design, 3 cells of the same size should be put in parallel. This saves one cell compared to the traditional lay-out. The efficiency of the cooler will be unaffected. The peak instantaneous power that is needed may be higher for the configuration with 3 parallel cells as all 3 cells can be in the heating phase at the same time. An alternative is to use a single-cell that is three times larger. This is simpler and more reliable compared to using 3 cells in parallel. When we assume that the chance of failures is determined by the compressor cells, the chance that the configuration with one large cell fails during its lifetime is three times smaller than that of the configuration with 3 parallel cells. If the heat capacity of the end caps of the compressor cells is negligible compared to that of the wall, which is typically the case for large length-to-diameter ratios, and when the temperature gradient over the sorber is negligible, the energy needed during the heating phases per gram of sorber material is unchanged. If the cool down time is also not affected, the efficiency of a compressor with a single large cell is the same as that with 3 parallel cells. If the cool down time is increased, the efficiency of the compressor with a single large cell will be lower as the produced mass flow rate is lower. The peak instantaneous input power will be the same for both designs. One can increase the reliability even further by placing a fourth cell parallel. Now 2 cells must fail before the compressor cannot meet its specifications anymore. When the chance that the compressor with 3 parallel cells fails during its lifetime is K, the chance that 1 of the 4 cells fail is $\frac{4}{3}K$, whereas the chance that 2 cells fail is $\frac{4}{3}K^2$. If K is e.g. 3%, then the failure chance reduces with a factor 25 when an additional cell is placed.

4.2. Implications for the cooler

When the compressor is connected to a LH cold stage, the variation of the pressure in the low-pressure buffer affects the temperature of the liquid in the boiler of the cold stage. In Fig. 7, the measured pressures from the

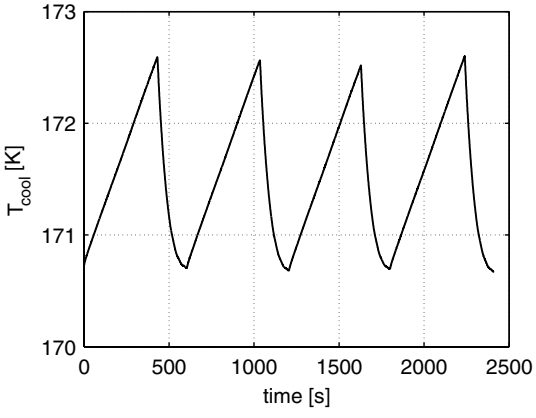

Fig. 7. Calculated temperature of the liquid in the boiler of a cold stage as derived from the pressure in the low-pressure buffer.

low-pressure buffer are converted to the temperature of the liquid within a boiler using GasPak [23]. This temperature varies between 170.7 and 172.6 K, a fluctuation of less than 2 K. Apart from common techniques to control a cooler's cold tip temperature, with this configuration one can reduce the variation by increasing the buffer volume size. Also the cooling power will vary somewhat because of the time-dependent flow through the cold stage and the pressure-dependent enthalpy of cooling. This will result in a variable liquid production rate, which in general is not a problem. Assuming a precooling temperature of 235 K and ideal counterflow heat exchangers, this configuration would give an average cooling power of 42 mW at about 172 K if a cold stage with ideal heat exchangers would be connected to the compressor. A larger cooling power can be obtained by faster cycling of the compressor, by using more cells in parallel, or by using larger cells as discussed in the previous section.

4.3. Sensitivity analysis

A sensitivity analysis was performed experimentally to investigate the effect of variations in the control parameters on the compressor behaviour. Four control parameters were investigated. These are described in Table 1. The setting for each control parameter was varied while the other parameters were kept constant. For each setting, the compressor was operated for at least 18 cycles. Only the last 10 cycles, during which the compressor was in stable operation, were taken into account.

The maximum amount of power that can be obtained from the created pressure difference, or the exergy rate, is [24]

$$\dot{W}_{\max} = -\frac{\mathrm{d}(U - T_{\mathrm{HS}}S)}{\mathrm{d}t} + \dot{m}_{\mathrm{H}}(h_{\mathrm{H}} - T_{\mathrm{HS}}s_{\mathrm{H}}) - \dot{m}_{\mathrm{L}}(h_{\mathrm{L}} - T_{\mathrm{HS}}s_{\mathrm{L}}) \quad (2)$$

with U the internal energy and S the entropy of the gas in the system to which the pressure difference is applied, T_{HS} the heat sink temperature, $\dot{m}$ the mass flow, h the specific enthalpy, and s the specific entropy of the gas. The subscript H refers to conditions of the gas at the high-pressure side, whereas an L refers to the low-pressure side of the compressor. We calculated the average of the maximum available power during a cycle by summation of the averages of the individual terms of Eq. (2). As the compressor is in stable operation, the mean of the first term right to the equal sign is zero. For the calculation we assumed that the high-pressure gas is cooled to the heat sink temperature before it comes available to a system that converts the pressure difference to work or cooling power. For $\dot{m}_{\mathrm{H}}$ the mass flow through mass flow meter B (see Fig. 5) was taken whereas the flow measured by mass flow meter C was taken for $\dot{m}_{\mathrm{L}}$. Note that the position of the mass flow sensors, or in other words the boundary of the system that converts the available pressure difference to work, affects the values that are obtained for the exergy. The sizes of the volumes between the flow sensors and the restriction affect the flow through the sensors even when the volumes of the buffers remain unaltered. This influences the rate of exergy as the pressures in the buffers are not constant during a cycle.

Table 1
Control parameters that were varied in the sensitivity analysis

Parameter	Description
f_{BC}	$\frac{\dot{m}_{\mathrm{cell}\rightarrow\mathrm{HP_{buffer}}}}{\dot{m}_{\mathrm{restr}}}$ upon switching from heating to cooling mode
f_{DA}	$\frac{\dot{m}_{\mathrm{LP_{buffer}}\rightarrow\mathrm{cell}}}{\dot{m}_{\mathrm{restr}}}$ upon switching from cooling to heating mode
P_{input}	Peak heater power (W)
$T_{\max}$	compressor set maximum temperature (K)

The compressor COP results from

$$\mathrm{COP} = \frac{\overline{\dot{W}_{\max}}}{\overline{P_{\mathrm{input}}}} = \frac{\int_{\mathrm{cycle}} \dot{m}_{\mathrm{H}}(h_{\mathrm{H}} - T_{\mathrm{HS}}s_{\mathrm{H}})\,\mathrm{d}t - \int_{\mathrm{cycle}} \dot{m}_{\mathrm{L}}(h_{\mathrm{L}} - T_{\mathrm{HS}}s_{\mathrm{L}})\,\mathrm{d}t}{\int_{\mathrm{cycle}} P_{\mathrm{input}}\,\mathrm{d}t} \quad (3)$$

Only the input power for the heater was taken into account. The power needed to actuate the gas-gap was excluded.

4.3.1. Variation of f_{BC}

The compressor cell was operated with f_{BC} set to values between 0.5 and 4. The other settings were as described in Section 4.1. Fig. 8 shows the variation of pressures, mass flows, rate of exergy and compressor COP with f_{BC}. The effective value of f_{BC} is not the same as the factor that was set in the control software. The intermittent heating causes an oscillating flow from the cell to the buffer. The software switches the heater off as soon as the flow drops below $f_{\mathrm{BC}} \cdot \dot{m}_{\mathrm{restr}}$. This will always be near the minimum of the oscillations. The average flow to the high-pressure buffer at this moment will be higher. Besides, when the software detects that heating should be stopped, it takes some time before the compressor cell starts cooling down and the high-pressure check valve closes. We are interested in the factor f_{BC} just before this happens. To take these effects into account, the 'effective' value of f_{BC} was estimated by averaging the flow between the cell and the high-pressure buffer during the last two oscillations and dividing this over the flow through the restriction. The values for the individual cycles were averaged. In the figure, the standard deviation was plotted as the error.

When increasing f_{BC}, i.e. switching sooner, both the amount of gas that flows from the cell to the high-pressure buffer during a cycle and the cycle time reduce. The pressure swing of the compressor, i.e. the difference between high pressure and low pressure, depends on the amount of gas the compressor pumps per unit of time. At low values of f_{BC}, the pressure swing increases with increasing f_{BC}, because the cycle time reduces more rapidly than the amount of gas. When f_{BC} is increased further, the amount of gas reduces faster than the cycle time, resulting in a decreasing pressure swing. Note that the change in pressure swing caused by the

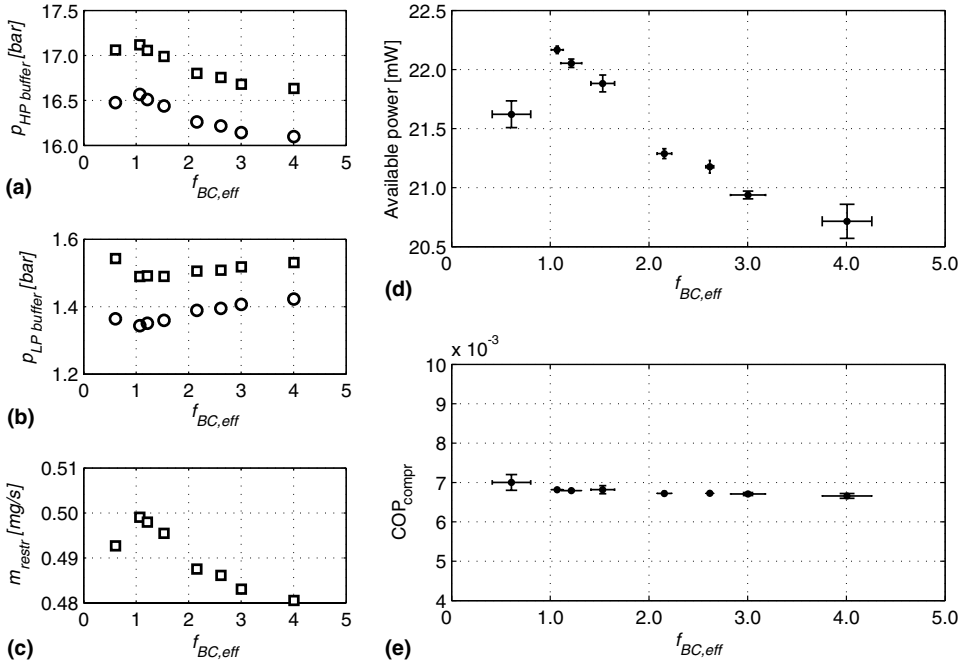

Fig. 8. Behaviour of sorption compressor cell with variation of f_{BC}. The standard deviations in pressures and mass flows are smaller than 1%. (a) Maximum and minimum observed pressure in the high-pressure buffer. (b) Similar for the low-pressure buffer. (c) Mass flow through the restriction. (d) Available power, averaged over a cycle. (e) Compressor efficiency.

variations in f_{BC} is relatively small. The difference between the minimum and maximum pressures in the low-pressure buffer decreases with increasing values of f_{BC}. The cycle time goes down, mainly due to the shorter duration of phase B, while the length of phase D remains fairly constant. This results in a reduction in the pressure variation in the low-pressure buffer (see Eq. (1)), whereas the pressure variation in the high-pressure buffer is negligible.

The mass flow through the restriction depends on the pressure difference between the high- and low-pressure buffers. During a cycle, the fluctuations in mass flow, high pressure, and low pressure are relatively small. In the regime the compressor is operating, xenon is a near-ideal gas. Then, $|\Delta h| \ll |T\Delta s|$ and the available power roughly equals $-\dot{m}T_{HS}\Delta s$. A larger pressure swing results in both a larger flow and a larger entropy difference between the gas that flows out off and into the compressor. So, the rate of exergy increases as the pressure difference increases. Note that the effect of f_{BC} on the magnitude of the available power is small. From Fig. 8(e) it turns out that the compressor COP slightly decreases for increasing values of f_{BC}. Apparently, the input power decreases slower than the exergy. The maximum pressure difference is achieved for f_{BC} is equal to or slightly larger than 1.

4.3.2. Variation of f_{DA}

The compressor is switched from the cooling mode to the heating mode when the flow from the low-pressure buffer to the cell falls below $f_{DA} \cdot \dot{m}_{restr}$. The effect of a change in f_{DA} on the compressor operation was investigated. The results are shown in Fig. 9. When the software switches the compressor to the heating mode, it takes some time before the pressure in the cell builds up and the low-pressure check valve closes. As we are interested in the flow just before the check valve closes and not in f_{DA} at the moment the software performs the switch, a correction on f_{DA} is needed. As there are no oscillations in the relevant flows, the correction factor is much smaller than for f_{BC}. At the moment the check valve closes, there is a distinct discontinuity in the derivative of the flow. The effective value of f_{DA} was calculated by dividing the mass flow to the cell by the mass flow through the restriction just before this discontinuity. The standard deviations of the thus obtained effective values are smaller than 3%.

Similar to the study of changes in f_{BC}, an increase in f_{DA} reduces both the cycle time and the amount of gas that is pumped by the compressor during a cycle. For low values of f_{DA}, the cycle time reduces faster than the amount of gas that is pumped. For larger values, the amount of gas reduces faster as the length of phase D becomes small compared to the lengths of the other phases. The latter hardly change with f_{DA}. This also explains why the pressure variation in the low-pressure buffer is barely affected by f_{DA}, whereas the variation in the high-pressure buffer changes considerably.

The total amount of exergy (in Joules) that is produced during a cycle decreases for increasing values of f_{DA}: the *average* rate of exergy hardly changes (see Fig. 9(d)) whereas the cycle time reduces dramatically. The total amount of heat input for each cycle is roughly constant as f_{BC} is fixed. Therefore, the compressor COP reduces as f_{DA} increases as is confirmed by Fig. 9(e).

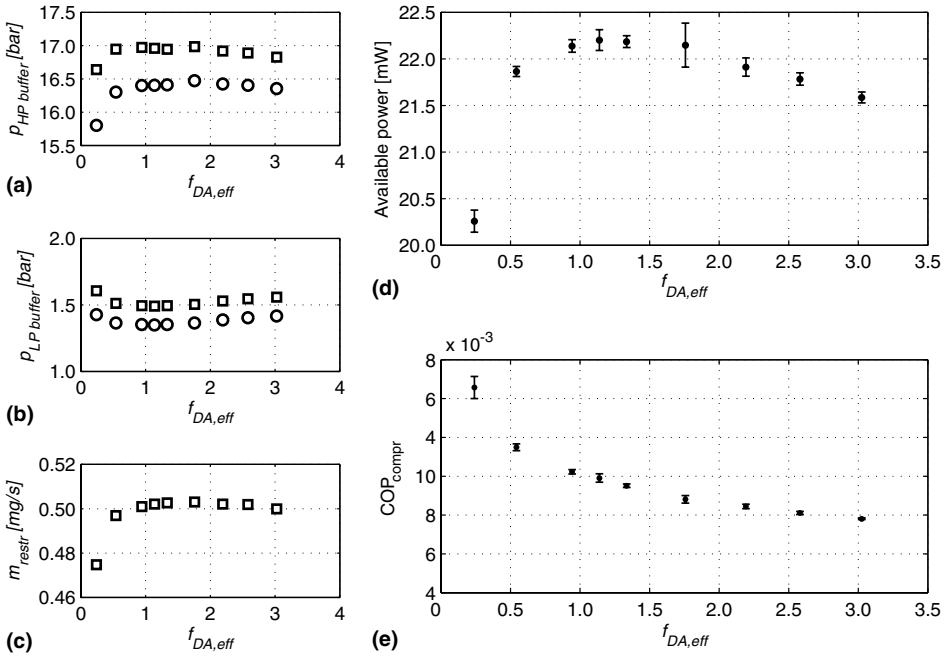

Fig. 9. Behaviour of sorption compressor cell with variation of f_{DA}. The standard deviation is smaller than 1% for all pressures and mass flows. (a) Maximum and minimum observed pressure in the high-pressure buffer. (b) Similar for the low-pressure buffer. (c) Mass flow through the restriction. (d) Maximum available power, averaged over a cycle. (e) Compressor efficiency.

4.3.3. Variation of input power

The *average* input power to the compressor can be changed by altering the duty cycle or by varying the voltage over the thermocouple. For the sensitivity analysis, the voltage over the thermocouple was varied whereas the control algorithm was not changed. The results are shown in Fig. 10. For the lowest input powers that were applied, the compressor cell does not reach the set maximum temperature, and an increase in heating power results in an increase in the highest temperature that the compressor cell reaches. This has a positive effect on the amount of gas that comes off the sorber. On the other hand, also the tempera-

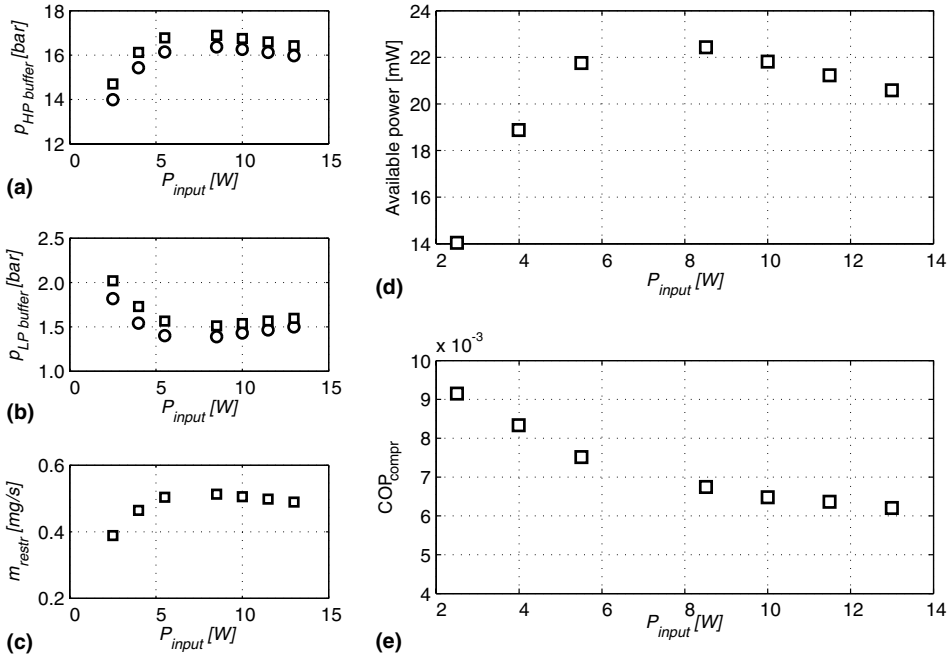

Fig. 10. Effect of variation in the peak heater input power on: (a) Pressure in high-pressure buffer. (b) Pressure in the low-pressure buffer. (c) Mass flow through the restriction. (d) Maximum available power, averaged over a cycle. (e) compressor COP. The standard deviations are smaller than 1% for all pressures and mass flows.

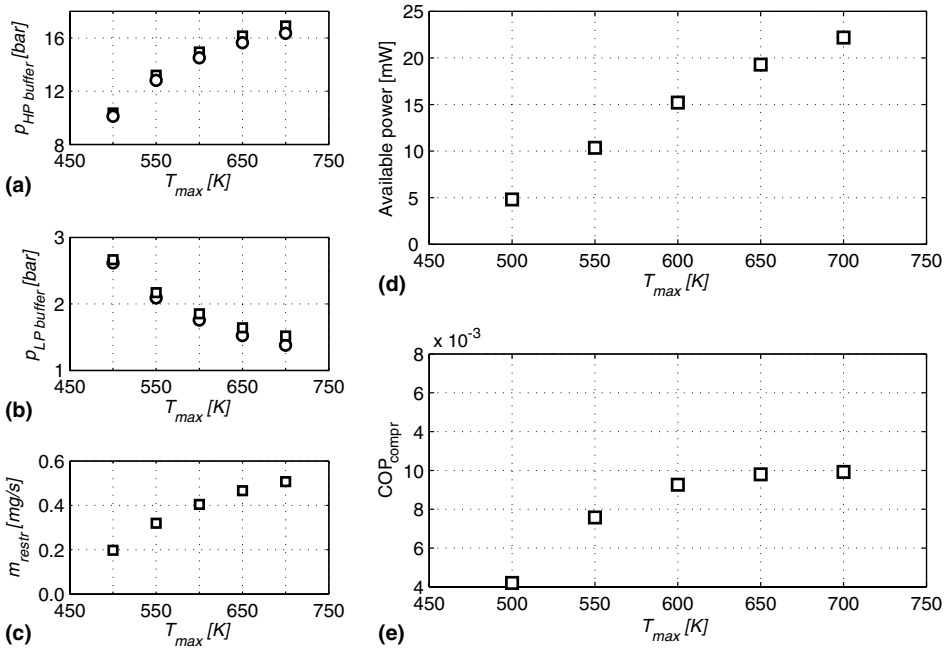

Fig. 11. Effect of variation on the set maximum temperature on: (a) pressure in high-pressure buffer, (b) pressure in the low-pressure buffer, (c) mass flow through the restriction, (d) maximum available power, averaged over a cycle, (e) compressor COP. The standard deviations are smaller than 1% for all pressures and mass flows.

ture gradient over the sorber material becomes larger. As $\partial^2 x_s/\partial T^2$ is positive, this has a negative effect on the total amount of gas that is desorbed. The combined effect is that the amount of gas that is pumped in a single cycle reduces slightly for increasing input powers. A larger input power also reduces the length of the heating phases. For low input powers, the heating phases are dominant in the cycle time, so the total cycle time reduces significantly when the heating power is increased. As the cycle time reduces faster than the total amount of gas that is pumped during a cycle, the pressure swing increases.

For input powers of 5.5 W and above, the compressor cell reaches the set maximum temperature of 700 K and the control algorithm reduces the time-averaged input power during the heating phase. It turns out that less gas is pumped from the cell to the buffer while at the same time the cycle time goes down. The reduction in the cycle time is comparable to the reduction in the amount of gas that is pumped. The overall effect is a moderate reduction of the pressure swing. To achieve a high compressor COP, a low input power is beneficial because of the lower temperature profile.

4.3.4. Variation of set maximum temperature

The set maximum temperature was changed from 500 to 700 K in steps of 50 K. The results are shown in Fig. 11. A higher maximum temperature implies a larger heat input. As the heating power is not changed, the heating phases take longer, resulting in longer cycle times. A higher cell temperature also means that more gas comes off the sorber. As a result, the amount of mass that is cycled per unit of time increases when the maximum temperature is increased. The pressure swing increases less than linear with the set maximum temperature as $\partial^2 x_s/\partial T^2$ is positive. So, the increase in amount of desorption goes down, whereas the cycle time increases about linearly. The total heat input increases somewhat faster than the gain in available power. From the figure, it turns out that the optimum compressor COP is obtained for a set maximum temperature of about 700 K.

4.3.5. Conclusions of sensitivity analysis

For the given compressor design and control algorithm, the maximum pressure swing is obtained for effective values of f_{BC} and f_{DA} slightly above 1, a peak input power of about 7 W, and a set maximum temperature above 700 K. The effect of a change in the set maximum heater temperature and the input power on the achieved pressure swing is much larger than that of a change in f_{BC} or f_{DA}. The optimum in the maximum available power roughly coincides with the maximum in the pressure swing. An optimum compressor COP is achieved for low values of f_{BC} and f_{DA}, a low heater input power, and a set maximum temperature of about 700 K. However, for small values of f_{BC} and f_{DA}, the available power goes to zero. The influence of changes in f_{BC} and f_{DA} around the values that give the maximum power is very small.

5. Conclusions

An alternative sorption compressor design, consisting of a single compressor cell, two check valves, and two buffer

volumes, was investigated. Such a design is easier to operate than a compressor consisting of multiple cells that operate out of phase. It is less complex and increases the reliability of the cooler. The principle was demonstrated using a set-up with a sorption compressor of about 8 cm^3 that was filled with Maxsorb activated carbon. Xenon was used as the working gas. A continuous flow of 0.52 mg/s was established with a pressure swing of 1.39–17.0 bar. If the compressor would be connected to a JT expansion stage, we expect a cooling power of about 42 mW at 172 K.

The effect of the control parameters f_{BC}, f_{DA}, the maximum heater temperature, and the peak input power on the compressor operation were experimentally investigated. From the sensitivity analysis, it appears that the effect of the set maximum heater temperature and the input power on the achieved pressure swing is much larger than that of a change in f_{BC} or f_{DA}. An optimum compressor COP is achieved for low values of f_{BC} and f_{DA}, a low input power, and a set maximum temperature of about 700 K. However, for small values of f_{BC} and f_{DA}, the power goes to zero.

Acknowledgement

This research was supported by the MESA + research institute of the University of Twente.

References

[1] The Kansai Coke & Chemicals Co. Ltd., 1-1 Oh-Hama, Amagasaki, Japan 660.
[2] Bowman Jr RC, Kiehl B, Marquardt E. Spacecraft thermal control handbook, vol. 2. El Segundo (CA): The Aerospace Press; 2003. p. 187–216 [chapter 10].
[3] Duband L. Etude et réalisation d'une machine frigorifique à cycle de Joule–Thomson, utilisant un compresseur thermique à adsorption. USTM Grenoble 1987.
[4] Suhanan, Duband L, Ravex A, Feidt ML. Etude expérimentale d'un réfrigérateur Azote à cycle Joule Thomson à adsorption, in: XIXth international congress of refrigeration, vol. IIIb, 1995. p. 1247–55.
[5] Bard S. Improving adsorption cryocoolers by multi-stage compression and reducing void volume. Cryogenics 1986;26:450–8.
[6] Burger JF, Holland HJ, Wade LA, ter Brake HJM, Rogalla H. Thermodynamic considerations on a microminiature sorption cooler. Cryocoolers 10. New York: Kluwer Academic/Plenum Publishers; 1999. p. 553–63.
[7] Marlow Industries, Inc., 10451 Vista Park Road, Dallas, TX, USA. Available from: http://www.marlow.com.
[8] Otowa T, Tanibata R, Itoh M. Production and adsorption characteristics of MAXSORB: high-surface-area active carbon. Gas Separat Purif 1993;7(3):241–5.
[9] Omega Engineering, Inc., One Omega Drive, Stamford, Connecticut 06907-0047, P.O. Box 4047, USA. Available from: http://www.omega.com.
[10] Burger JF, Holland HJ, ter Brake HJM, Elwenspoek M, Rogalla H. Construction and operation of a 165 K microcooler with a sorption compressor and a micromachined cold stage. Cryocoolers 12. New York: Kluwer Academic/Plenum Publishers; 2003. p. 643–9.
[11] Kulite Semiconductor Products, Inc., One Willow Tree Road, Leonia, NJ 07605, USA. Available from: http://www.kulite.com.
[12] Heraeus Sensor Technology GmbH, Reinhard-Heraeus-Ring 23, D-63801 Kleinostheim, Germany. Available from: http://heraeus-sensor-technology.de.
[13] Corruccini RJ. Gaseous heat conduction at low pressures and temperatures, Vacuum VII and VIII, 1957–1958, p. 19–29.
[14] Roth A. Vacuum technology. Amsterdam: Elsevier Science; 1990.
[15] Burger JF, Holland HJ, van Egmond H, Elwenspoek M, ter Brake HJM, Rogalla H. Fast gas-gap heat switch for a microcoolers. Cryocoolers 10. New York: Kluwer Academic/Plenum Publishers; 1999. p. 565–74.
[16] Prina M, Kulleck JG, Bowman Jr RC. Assessment of Zr–V–Fe getter alloy for gas-gap heat switches. J Alloys Compd 2002;330–332:886–91.
[17] MKS Instruments, 90 Industrial Way, Wilmington, Massachusetts 01887, USA. Available from: http://www.mksinst.com.
[18] Swagelok Company, 29500 Solon Road, Solon, OH 44139, USA. Available from: http://www.swagelok.com.
[19] Burger JF, van der Wekken MC, Berenschot E, Holland HJ, ter Brake HJM, Rogalla H. High pressure check valve for application in a miniature cryogenic sorption cooler, in: Twelfth IEEE international conference on micro electro mechanical systems, 1999. p. 183–8.
[20] National Instruments Corporation, 11500 N MoPac Expwy, Austin, TX 78759-3504, USA. Available from: http://www.ni.com.
[21] Druck Ltd., Fir Tree Lane, Groby, Leicester, LE6 0FH, England. Available from: http://www.druck.com.
[22] Bronkhorst High-Tech BV, Nijverheidsstraat 1A, 7261 AK, Ruurlo, The Netherlands. Available from: http://www.bronkhorst.nl.
[23] Cryodata Inc., P.O. Box 558, Niwot, CO 80544, USA. Available from: http://www.cryodata.com.
[24] Bejan A. Advanced engineering thermodynamics. Wiley Interscience; 1988.